Global Assessment of Regulation of Phosphorylation of Insulin Receptor Substrate (IRS)-1 by Insulin *in Vivo* in Human Muscle

Received for publication 22 September 2006 and accepted in revised form 8 March 2007.

Zhengping Yi*[1,2], Paul Langlais*[1,3], Elena A. De Filippis*[1,2], Moulun Luo*[1,2], Charles R. Flynn[1], Stefanie Schroeder[1], Susan T. Weintraub[4], Rebekka Mapes[1,5], and Lawrence J. Mandarino[1,2,3]

[1]Center for Metabolic Biology, Arizona State University, Tempe, Arizona; [2]School of Life Sciences, Arizona State University, Tempe, Arizona; [3]Department of Kinesiology, Arizona State University, Tempe, Arizona; [4]Department of Biochemistry, The University of Texas Health Science Center, San Antonio, Texas; [5]Department of Physiology, The University of Texas Health Science Center, San Antonio, Texas

*Contributed equally to this work.

Address for Correspondence:

Lawrence J. Mandarino, Ph.D.
Director, Center for Metabolic Biology
College of Liberal Arts and Sciences
PO Box 873704
Tempe, Arizona 85287-3704
U.S.A.
Email: lawrence.mandarino@asu.edu

Additional information for this article can be found in an online appendix at http://diabetes.diabetesjournals.org.

Abstract

Objective. Research has focused on Insulin Receptor Substrate-1 (IRS-1) as a locus for insulin resistance. Tyrosine phosphorylation of IRS-1 initiates insulin signaling; serine/threonine phosphorylation alters the ability of IRS-1 to transduce the insulin signal. Of 1242 amino acids in IRS-1, 242 are serine/threonine. Serine/threonine phosphorylation of IRS-1 is affected by many factors, including insulin. The purpose of this study was to perform global assessment of phosphorylation of serine/threonine residues in IRS-1 *in vivo* in humans.

Research Design and Methods. In this report we describe our use of capillary HPLC-electrospray tandem mass spectrometry to identify/quantify site-specific phosphorylation of IRS-1 in human *vastus lateralis* muscle obtained by needle biopsy, basally and after insulin infusion in four healthy volunteers.

Results. Twenty-two serine/threonine phosphorylation sites were identified; fifteen were quantified. Three sites had not been identified previously (Thr^{495}, Ser^{527}, and S^{1005}). Insulin increased the phosphorylation of Ser^{312}, Ser^{616}, Ser^{636}, Ser^{892}, Ser^{1101}, and Ser^{1223} (2.6 ± 0.4, 2.9 ± 0.8, 2.1 ± 0.3, 1.6 ± 0.1, 1.3 ± 0.1, and 1.3 ± 0.1 fold, respectively, compared to basal; $P < 0.05$); phosphorylation of Ser^{348}, Thr^{446}, Thr^{495}, and Ser^{1005} decreased (0.4 ± 0.1, 0.2 ± 0.1, 0.1 ± 0.1, and 0.3 ± 0.2 fold, respectively; $P < 0.05$).

Conclusions. These results provide an assessment of IRS-1 phosphorylation *in vivo* and show that insulin has profound effects on IRS-1 serine/threonine phosphorylation in healthy humans.

Introduction

Through the efforts of a large number of investigators, many of the details of insulin signaling have been defined on a molecular level (1). Despite this, the changes in insulin signaling that produce insulin resistance *in vivo* in tissues such as skeletal muscle, adipose tissue, or liver, remain, for the most part, unknown. Numerous defects have been identified in skeletal muscle from insulin resistant obese or type 2 diabetic patients, including decreased insulin activation of the insulin receptor beta subunit, reduced tyrosine phosphorylation of Insulin Receptor Substrate-1 (IRS-1), and dampened binding of the p85 regulatory subunit of phosphatidylinositol 3'-kinase (PI 3'-kinase) and association of PI 3'-kinase activity with IRS-1 (2,3).

Due to the central and multifaceted role of IRS-1 in insulin signaling, recent research has focused on IRS-1 as a locus for insulin resistance. Human IRS-1 (hIRS-1) is a 1242-amino acid protein of predicted molecular weight of 132 kDa that migrates in electrophoretic gels at an apparent size of 185 kDa, due to extensive phosphorylation (4). IRS-1 is phosphorylated by the insulin receptor tyrosine kinase at a number of tyrosine residues that serve as recognition sites for Src homology-2 (SH-2) domain-containing proteins, such as the p85 regulatory subunit of PI 3'-kinase, that transmit the insulin signal. In addition, of the 1242 amino acids that compose IRS-1, 182 are serine and 60 are threonine residues. Many of these are in known consensus kinase motifs, and, even under basal, non-stimulated conditions, IRS-1 is heavily phosphorylated. A number of serine/threonine phosphorylation sites have been identified, and a few of these have been characterized for function (5-19). Some sites, such as Ser^{1223}, appear to be positive modulators of IRS-1 function (13), whereas others, such as Ser^{312} and Ser^{636}, have been identified primarily to have a dampening effect (5,15). Some sites, such as Ser^{323} (Ser^{318} in rodents) can have both a positive and a negative function (20).

Ser^{312} (Ser^{307} in the mouse IRS-1 sequence) has drawn attention since phosphorylation at this site interferes with association of the adjacent phosphotyrosine-binding (PTB) domain of IRS-1 with the tyrosine-phosphorylated insulin receptor (5). Ser^{312} can be phosphorylated by kinases, such as c-jun N-terminal kinase (JNK) and inhibitor kappa B kinase (IKK), that are activated by inflammatory stimuli, including tumor necrosis factor-α (TNF-α) (5,7,9,12). Increased phosphorylation of Ser^{312} has been implicated in inflammation and lipid-induced insulin resistance, as well as insulin resistance associated with polycystic ovary disease (21,22).

Although there is strong evidence that Ser^{312} is likely to be involved in insulin resistance, the existence of a large number of other serine and threonine residues that are phosphorylated suggest that IRS-1 function is modulated in a complex manner by phosphorylation that can cause positive or negative effects. The net result of serine/threonine phosphorylation may depend upon the pattern and time course of phosphorylation of combinations of residues. Although several specific antibodies to IRS-1 phosphorylation sites are available, to date there have been no methods published to globally assess the level and pattern of serine/threonine phosphorylation of this protein in human tissues.

The insulin-induced mobility shift on SDS-PAGE gels observed with IRS-1 immunoprecipitated from homogenates of human muscle biopsies suggests that insulin itself alters IRS-1 serine/threonine phosphorylation (2), and this insulin-induced phosphorylation of IRS-1 conceivably could affect its subsequent function. Phosphorylation of some sites, such as Ser^{1223}, is increased in response to insulin, and this is reported to have positive regulatory effects on IRS-1 function (13). Such phosphorylation events could have a positive

or "feed-forward" effect that enhances insulin signaling. Phosphorylation of other sites, such as Ser^{312}, if increased *in vivo* in humans in response to insulin, could have a negative feedback function and desensitize insulin signaling. In adipocytes, insulin-stimulated phosphorylation of IRS-1 targets it for ubiquitination and degradation by proteasomes, contributing to downregulation of insulin signaling (23). Therefore, increased knowledge of the regulation of IRS-1 serine/threonine phosphorylation *in vivo* in humans could lead to a better understanding of insulin signaling and insulin resistance.

We previously developed and validated a hypothesis-driven mass spectrometry-based approach for quantifying relative changes in phosphorylation of IRS-1 at many sites at the same time in the same biological sample (19). We now report on our adaptation of this method for relative quantification of serine/threonine phosphorylation of endogenous IRS-1 immunoprecipitated from small, percutaneous biopsies of human *vastus lateralis* muscle. We used this method to quantify relative changes in a large number of serine/threonine residues phosphorylated *in vivo* in response to an insulin infusion (euglycemic, hyperinsulinemic clamp) in healthy volunteers. It is reasonable to anticipate that this method can be applied to relative quantification of phosphorylation sites on any protein that can be immunopurified from small tissue samples.

Methods

Subjects. Four lean, healthy individuals without a family history of type 2 diabetes took part in the study. None of the subjects had any significant medical problems and their weight was stable for at least 3 months prior to the study. No subject was taking any medications known to affect glucose metabolism. None of the subjects participated in any heavy exercise and they were instructed and not to engage in vigorous exercise for at least 3 days before the study. The purpose, nature and potential risks of the study were explained to all subjects and written consent was obtained before their participation. The protocol was approved by the Institutional Review Board of Arizona State University. All subjects received a 75-g oral glucose tolerance test on a separate day to confirm normal glucose tolerance (OGTT).

OGTT. Baseline blood samples for determination of plasma glucose, free fatty acid (FFA), and insulin concentrations were drawn at -30, -15 and 0 min. At time zero, subjects ingested 75 g of glucose in 300 ml of orange-flavored water. Plasma glucose, FFA, and insulin concentrations were measured at 15-min intervals for 2 hr.

Euglycemic clamp with muscle biopsies. A euglycemic, hyperinsulinemic clamp was used to assess insulin sensitivity and expose skeletal muscle to insulin *in vivo*, as previously described (2,24). On the day of study, at 0700 hr (-120 min), a catheter was placed in an antecubital vein and maintained throughout the study for infusions of insulin and glucose. A second catheter was placed in a retrograde manner into a vein on the back of the hand, which was then placed in a heated box (60 °C). Baseline arterialized venous blood samples for determination of plasma glucose and insulin concentrations were drawn at -30, -20, -10, -5, and 0 min. At 0800 h (time -60 min), after resting for 60 min, a percutaneous needle biopsy of the *vastus lateralis* muscle was performed under local anesthesia (2). At 0900 hr (0 min), a primed, continuous infusion of human regular insulin (Novolin, Novo Nordisk Pharmaceuticals, Princeton, NJ) was started at a rate of 80 $mU \cdot min^{-1} \cdot m^{-2}$ body surface area and continued for 120 min. Arterialized blood samples were collected every 5 min for plasma glucose determination and a 20% glucose infusion was adjusted to maintain the plasma glucose concentration at each subject's fasting plasma glucose level. Throughout the insulin clamp, blood samples for determination of plasma glucose concentration were drawn every 5 min, and blood samples for determination of plasma

insulin were collected every 10-15 min. At time 1100 hr (+120 min after the start of insulin infusion) a second percutaneous muscle biopsy was obtained from the contralateral *vastus lateralis* muscle. Visible fat and/or connective tissue were removed and the samples (100 – 150 mg each) were frozen in liquid nitrogen for subsequent analyses.

Analytical determinations. Plasma glucose was measured by the glucose oxidase method (Beckman Instruments, Fullerton, CA). Plasma insulin concentration was measured by radioimmunoassay (Diagnostic Products Corporation, Los Angeles, CA).

Muscle biopsy processing. Frozen muscle biopsies were homogenized in detergent-containing lysis buffer as described (2). Protein concentrations were determined by the method of Lowry (25).

Immunoprecipitation, gel electrophoresis, and immunoblotting. IRS-1 was immunoprecipitated from muscle lysates as described (2). For mass spectrometry analysis, 1 to 5 mg of total protein was immunoprecipitated, whereas for immunoblot analysis, 0.3 mg was used for IRS-1 protein blots and 1.0 mg was used for each anti-phosphoserine blot. Immunoprecipitated proteins were resolved on 7.5% SDS polyacrylamide gels. For mass spectrometry analysis, gels were stained with Coomassie blue for protein visualization, and the gel area corresponding to the position of IRS-1 was excised and processed as described below. No IRS-1 band was visible with either Coomassie blue or the more sensitive SYPRO Ruby stain because of the low abundance of IRS-1 in human muscle samples. For immunoblot analysis, proteins were transferred electrophoretically from the gel to nitrocellulose membranes. Anti-IRS-1, anti-phospho-IRS-1-Ser^{312} (Upstate Biotechnology, Inc., Lake Placid, NY), anti-phospho-IRS-1Ser$^{636/639}$ (Cellular Signaling Technologies, Danvers, MA) and anti-phosphotyrosine (PY99, Santa Cruz Biotechnology, Inc., Santa Cruz, CA) antibodies were obtained commercially.

In-gel digestion. The gel portions containing IRS-1 were excised, placed in a 0.6-ml polypropylene tube, washed with 400 µl of 40 mM NH_4HCO_3, destained twice with 300 µl of 50% acetonitrile (ACN) in 40 mM NH_4HCO_3 and dehydrated with 100% ACN for 15 min. After removal of ACN by aspiration, the gel pieces were dried in a vacuum centrifuge at 60 °C for 20 min. Trypsin (250 ng; Sigma Chemical Co., St. Louis, MO) in 20 µl of 40 mM NH_4HCO_3 was added, and the samples were maintained at 4 °C for 15 min prior to the addition of 50 µl of 40 mM NH_4HCO_3 containing 10 fmol/µl angiotensin II (Ang II; internal peptide reference). The digestion was allowed to proceed at 37 ºC overnight and was terminated by addition of 10 µl 5% formic acid (FA). After further incubation at 37 °C for 30 min and centrifugation for 1 min, each supernatant was transferred to a clean polypropylene tube. The extraction procedure was repeated using 40 µl of 5% FA, and the two extracts were combined. The resulting peptide mixtures were purified by solid-phase extraction (C18 ZipTip, Millipore, Billerica, MA) after sample loading in 0.05% heptafluorobutyric acid:5% FA (v/v) and elution with 50 % ACN:1% FA (v/v). The samples were dried by vacuum centrifugation, and 4 µl of 0.1% FA:2%ACN (v/v) was added.

Mass spectrometry. HPLC-ESI-MS^n was performed on a hybrid linear ion trap (LTQ)-Fourier Transform Ion Cyclotron Resonance (FTICR) mass spectrometer (LTQ FT, Thermo Fisher ; San Jose, CA) fitted with a PicoView™ nanospray source (New Objective, Woburn, MA). The mass spectrometer was calibrated weekly according to manufacturer's instructions, achieving mass accuracies of the calibrants within 2 ppm. For HPLC-ESI-MS/MS analyses of tryptic digests of hIRS-1, the mass values of the added Ang II internal standard were routinely within 3 ppm of theoretical. On-line capillary HPLC

was performed using a Michrom BioResources Paradigm MS4 micro HPLC (Alburn, CA) with a PicoFrit™ column (New Objective; 75 μm i.d., packed with ProteoPep™ II C18 material, 300 Å); mobile phase, linear gradient of 2 to 27% ACN in 0.1 % FA in 45 min, a hold of 5 min at 27% ACN, followed by a step to 50% ACN, hold 5 min and then a step to 80%; flow rate, 250 nl/min.

A "top-10" data-dependent tandem mass spectrometry (MS) approach was utilized to identify IRS-1 peptides and to obtain their HPLC retention times. In a top-ten scan protocol, a full scan spectrum (survey scan) is acquired followed by collision-induced dissociation (CID) mass spectra of the 10 most abundant ions in the survey scan. Use of this type of scan strategy results in acquisition of CID spectra of the ten most abundant ions appearing at any given time in an HPLC run. Thus, a large number of tandem mass spectra are acquired during the course of each analysis. For the experiments used in the current report, the survey scan was acquired using the FTICR mass analyzer in order to obtain high mass accuracy data. From this initial analysis, a list of potential phosphorylated peptides was generated based on detected serine/threonine-containing peptides of IRS-1. For localization of sites of phosphorylation, a scan protocol of 1 survey scan (FTICR), followed by 7 targeted MS/MS scans (CID spectra of specified *m/z* values that were acquired using the LTQ mass analyzer). For quantification, the following multi-segment strategy was employed: 1 survey scan, followed by 1 parent-list CID scan and 5 targeted CID scans. Ions in the parent list are only fragmented if they are detected above a specified minimum intensity; targeted ions are fragmented in each scan segment. Included in the parent list were the 1+ or 2+ charge states of six representative IRS-1 peptides selected from the prominent ions reproducibly observed in the top-10 data-dependent tandem-MS analysis (19,26). These peptides were used as internal standards for assessment of total, unphosphorylated, IRS-1 protein content (see below) and for relative quantification of phosphopeptides. The 2+ or 3+ ions of the phosphopeptides of interest were placed on the target list (19). In order to assess the relative quantities of a large number of phosphopeptides in each experiment and yet still maintain an acceptable mass analysis cycle times, the targeted *m/z* values were grouped into segments based on their expected HPLC retention times. All uninterpreted tandem MS data were searched against the human Swiss-Prot database using Mascot (Matrix Science, London, UK). Cross correlation of Mascot search results with X! Tandem was accomplished with Scaffold (Proteome Software; Portland, OR). Assignments of the phosphopeptides were confirmed by manual comparison of the tandem mass spectra with the predicted fragmentation generated *in silico* by the MS-Product component of ProteinProspector (http://prospector.ucsf.edu).

Peak areas for each peptide were obtained by integration of the appropriate reconstructed ion chromatograms (generated with a 5 ppm mass tolerance) for precursor ion masses acquired using the FTICR mass analyzer. The trace generated in a reconstructed ion chromatogram displays the intensity (abundance) of a specified ion relative to HPLC retention time in a format that is analogous to a UV absorbance trace for an HPLC/UV run. The peak areas for phosphopeptides then were normalized against the average peak area for six representative IRS-1 peptides (endogenous standards). Relative quantification of each phosphopeptide was obtained by comparing normalized peak-area ratios for obtained from IRS-1 isolated from muscle samples taken during basal and insulin-stimulated conditions (19). To determine variability, three equal (5-mg protein) aliquots of a homogenate of human muscle were separately immunoprecipitated. Immunoprecipitated proteins were resolved on gels, the portion of

the gel corresponding to IRS-1 was excised and digested with trypsin. The resulting peptides were subjected to HPLC-MS analysis as described. The coefficient of variation for the average of the six unphosphorylated IRS-1 peptides was found to be 12%. For the phosphopeptides observed and quantified in these preliminary experiments, coefficients of variation for Ser^{330}, Ser^{348}, Thr^{446}, Ser^{1100}, Ser^{1101}, and Ser^{1223} were 30, 9, 27, 5, 9, and 25%, respectively.

Statistical analyses. Statistical significance was assessed by comparing basal and insulin-stimulated phosphopeptide intensities (normalized to IRS-1 peptides as described above) using two-tailed paired t-tests.

Results

Subject characteristics and insulin-stimulated glucose metabolism. The characteristics of the subjects are given in Table 1. Subjects were lean (BMI = 24 $\pm$ 1.4 kg/m^2), aged 27 $\pm$ 4, and without a family history of type 2 diabetes mellitus. The rate of infusion of glucose required to maintain the subjects at euglycemia was 9.0 $\pm$ 0.9 mg/kg fat free mass/min at an insulin infusion rate of 80 $mU/min/m^2$ of body surface area, which produced plasma insulin concentrations of 506 ± 46 pmol/l At these insulin concentrations, endogenous glucose production in insulin-sensitive volunteers is completely suppressed, so the rate of glucose infusion can be taken as a measure of glucose disposal (27).

Identification of phosphorylation of IRS-1. Data-dependent capillary HPLC electrospray tandem mass spectrometry (HPLC-ESI-MS/MS) analysis of tryptic digests of proteins immunoprecipitated with an anti-IRS-1 antibody from skeletal muscle biopsies confirmed the presence of IRS-1. The sequence coverage of IRS-1 tryptic peptides detected in a representative data-dependent tandem MS analysis is shown in Figure 1. Due to the complexity of the tryptic digest of IRS-1 and the low abundance of IRS-1 in human muscle, no phosphopeptides were detected in a data-dependent analysis that did not include targeted or parent-ion list scans (see below). However, many IRS-1 peptides containing serine and/or threonine were detected. Since any peptide with serine or threonine has the potential to exist in a phosphorylated state, we predicted that low abundance phosphopeptides might be detected using a "targeted" MS scan strategy based on addition of 80 Da ($H_3PO_4 – H_2O$) to the mass of each detected IRS-1 peptide that contained serine or threonine. We constructed a hypothesis-driven strategy with various potential phosphopeptide *m/z* values in a target list, greatly improving efficiency for identifying phosphorylation. This approach enabled us to detect 22 distinct phosphorylation sites in 15 IRS-1 tryptic peptides. From Scaffold analysis of the database search results, 21 of the 22 phosphopeptides were identified at the 95% confidence level. The tandem mass spectrum of the peptide that did not generate a high-confidence identification in the Scaffold analysis ($IRS\text{-}1^{627\text{-}638}$ with phosphorylation on Ser^{636} and oxidation on Met^{633} and Met^{635}) matched that of a synthetic peptide that was identically phosphorylated and oxidized (not shown). Tandem mass spectra illustrating localization of the sites of phosphorylation for all phosphopeptides are given in Online Appendix 1. In three cases, a particular peptide was found to exist in more than one phosphorylated form. That is, multiple serines and/or threonines were present in the sequence and were found to be alternatively phosphorylated in individual monophosphorylated peptides (Table 2). In some cases, monophosphorylated peptide isoforms could not be resolved chromatographically but there was clear fragmentation data showing the presence of two or more monophosphorylated peptides in a chromatographic peak (Ser^{307}/Ser^{323}, Ser^{527}/Ser^{531}, and $Ser^{1142}/Ser^{1143}/Ser^{1145}$). In other cases, chromatographic separation of the monophosphorylated peptide isoform

pairs was possible (the peptides containing: Ser^{629} and Ser^{636}; Ser^{330} and Ser^{348}; the peptide containing Ser^{312} that was chromatographically distinct from the co-eluting mono-phosphorylated peptides containing Ser^{307} and Ser^{323}). The identified phosphopeptides contain a total of 70 serines and threonines, representing 29% of all serines and threonines in hIRS-1.

In our analyses of hIRS-1 from muscle biopsy tissue, we identified three new phosphorylation sites: Thr^{495}, Ser^{527}, and Ser^{1005}. We also detected a number of other phosphorylation sites (Ser^{307}, Ser^{312}, Ser^{323}, Ser^{330}, Ser^{348}, Thr^{446}, Ser^{531}, Ser^{574}, Ser^{616}, Ser^{629}, Ser^{636}, Ser^{892}, Ser^{1078}, Ser^{1100}, Ser^{1101}, Ser^{1142}, Ser^{1143}, Ser^{1145}, and Ser^{1223}) that have been reported previously by us and by other investigators using a variety of techniques, including site-directed mutagenesis, immunoblot analysis with site specific phospho-antibodies, and mass spectrometry (5,6,8,11,12,15-18,22).

Effect of insulin on IRS-1 phosphorylation. The effect of two hours of insulin infusion on the extent of phosphorylation of fifteen distinct phosphorylation sites was quantified by our analytical strategy (Table 2). Three additional peptides (Table 2) that contained multiple serine and threonine residues were found to exist in two or more individually phosphorylated forms (Ser^{307}/Ser^{323}, Ser^{527}/Ser^{531}, Ser^{1142}/Ser^{1143}/Ser^{1145}; see above, preventing individual quantification of these sites by mass spectrometry). The ion intensity for the added Ang II standard did not differ for basal or insulin-stimulated samples, indicating similar recoveries. Insulin infusion also had no statistically significant effect on the average ion intensity for the six unphosphorylated peptides used as internal IRS-1 standards, although there was an apparent tendency for a decrease of 29 ± 18% ($P = 0.34$) in the level of IRS-1 after insulin treatment. Reconstructed ion chromatograms for the six unphosphorylated IRS-1 peptides from basal and insulin-stimulated muscle biopsies are shown in Online Appendix 2.

The infusion conditions used for our study produced plasma insulin levels that were within the high physiological range. After two hours of insulin infusion, we found that relative phosphorylation of IRS-1 was increased at some sites and decreased at others when expressed relative to total IRS-1 protein as assessed by the six unphosphorylated IRS-1 peptides (Table 2). Phosphorylation of Ser^{312}, Ser^{616}, and Ser^{636} increased more than two fold in response to insulin ($P < 0.05$), while phosphorylation of Ser^{348}, Ser^{1005}, Thr^{446}, and Thr^{495} decreased significantly (Table 2). Phosphorylation was also found to be increased significantly at other sites by insulin, but to a lesser degree. For example, in the *C*-terminal portion of IRS-1, Ser^{1101} and Ser^{1223} both increased by 1.3 ± 0.1-fold during the two-hour insulin infusion (both $P < 0.05$). Representative reconstructed ion chromatograms for selected phosphopeptides that exhibited increased abundance ($pSer^{616}$), did not change ($pSer^{1078}$) or decreased ($pSer^{348}$) are shown in Figure 2 (top, middle and bottom panels, respectively). Figure 3 shows the chromatographic separation of ^{627}KGpSGDYMPMSPK^{638} ($pSer^{629}$) and ^{627}KGSGDYMPMpSPK^{638} ($pSer^{636}$) along with the corresponding tandem mass spectra identifying the specific sites of phosphorylation. Shown in Online Appendix 3 are reconstructed reaction chromatograms that validate the chromatographic separation of IRS-$1^{326-353}$ mono-phosphohorylated peptides containing $pSer^{348}$ and $pSer^{330}$.

Figure 4 provides a visual representation of the overall relative changes in phosphorylation of IRS-1; the regions where IRS-1 associates with the insulin receptor, the p85 regulatory subunit of PI 3'-kinase, and the tyrosine phosphatase SHP2 are also indicated in Figure 4. Fold changes are expressed as $\log_2$(fold change), so in Figure 4, a fold increase of 2.0 (100% increase) equates to

+1.0 and 0.5 of basal (50% decrease) corresponds to -1.0.

Insulin-induced changes in phosphorylation of Ser^{312} and Ser^{636}, determined by mass spectrometry analysis, were compared with immunoblot analysis using site-specific anti-phospho-antibodies directed against phospho-Ser^{312} and phospho-$Ser^{636/639}$ (Figure 5). As a positive control, we used an anti-phosphotyrosine antibody to detect insulin stimulation of tyrosine phosphorylation of IRS-1 (Figure 5). Using mass spectrometry analysis, a 2.6 ± 0.4-fold ($P < 0.05$) insulin-induced increase was found for phosphorylation at Ser^{312} and a 2.1 ± 0.3-fold ($P < 0.05$) increase at Ser^{636} (Table 2). Immunoblot analyses showed fold changes of 1.6 ± 0.5 and 1.3 ± 0.3 for Ser^{312} and $Ser^{636/639}$, respectively (not statistically significant).

Several other phosphorylation sites were found to be decreased following two hours of insulin infusion (see Figure 4). Except for Ser^{1005}, these sites all were within a 150-amino acid region of IRS-1 (residues 328 – 520) that lies proximal and *C*-terminal to the PTB domain (residues 161 – 264) that is responsible for association of IRS-1 with the insulin receptor. Phosphorylation at these sites (Ser^{348}, Thr^{446}, and Thr^{495}) decreased dramatically to 0.4 ± 0.1, 0.2 ± 0.1, and 0.1 ± 0.1 of basal values (all $P < 0.05$).

Discussion

The availability of genomics approaches for assessment of differences in global gene expression and proteomics techniques for determination of relative changes in abundance for a large number of proteins has made it possible to gain insight into highly complicated biological processes. Regulation of protein function by covalent modification(s) adds further complexity to these multidimensional systems. Development of methods for global assessment of posttranslational modifications of proteins has lagged behind other proteomics techniques. Quantification of posttranslational modifications of specific proteins isolated from small samples of human tissue is particularly challenging due to the extremely limited amount of protein available for analysis. The importance of modification of protein function/activity by phosphorylation has been known for decades. Phosphorylation of serine and threonine residues was recognized first as regulatory for protein activity, and later, tyrosine phosphorylation was established as playing a major role in the function of many proteins involved in cell signaling (28). Antibodies that recognize phosphorylated amino acids in specific amino acid sequence motifs have been developed as a way to use immunoblot analysis to obtain relative quantification of site-specific phosphorylation in proteins obtained from biological samples. Although these antibodies can be used very effectively for studies of selected regulatory sites (for example, Thr^{308} and Ser^{473} of Akt), they are much less useful for proteins such as IRS-1 in which there are a large number of known phosphorylation sites as well as numerous potential sites that may regulate the functions of this protein. In many cases, either the appropriate antibodies have not been generated or the available antibodies lack the requisite specificity. In addition, in our experience, antibodies that provide excellent results with lysates of cultured cells where proteins of interest often are over-expressed, frequently do not work as well in homogenates derived from biopsy specimens of human tissue. Moreover, even if site-specific antibodies were available for all phosphorylation sites identified here (which they are not), the immunoblot analyses would require more protein than would be obtainable from a single biopsy.

The results of the present study show that it is possible to assess relative changes in phosphorylation of many serine and threonine sites in IRS-1 immunoprecipitated from small (100 mg or less), percutaneous needle biopsies of human *vastus lateralis* muscle. Through coupling with the euglycemic

hyperinsulinemic clamp technique, we were able to study the *in vivo* regulation of 22 IRS-1 serine and threonine phosphorylation sites by insulin. To our knowledge, this is the first report of such an accomplishment. Of the 22 hIRS-1 phosphorylation sites reported here, three are new and previously unidentified in either *in vitro* or *in vivo* studies (Thr^{495}, Ser^{527}, and Ser^{1105}) and 20 are, for the first time, being reported and confirmed as phosphorylation sites *in vivo* [the two exceptions being Ser^{312} and Ser^{636}, both of which have been previously reported as phosphorylation sites *in vivo* (29,30)]. Numerous published reports have used *in vitro* kinase assays to identify potential kinases involved in IRS-1 phosphorylation as well as their respective sites, although data regarding whether these sites undergo phosphorylation in either cells or *in vivo* is lacking. Here, we confirm that, in fact, sites such as Ser^{307} and Ser^{330} [shown to be phosphorylated *in vitro* by Protein Kinase C (PKC)δ/PKCθ/Akt and Akt, respectively (31,32)], Ser^{574} [an *in vitro* substrate of PKCδ, PKCζ, and PKA (31)], and Ser^{1100}, Ser^{1142}, and Ser^{1143} [phosphorylated *in vitro* by PKA (26)] are genuine *in vivo* IRS-1 phosphorylation sites. Our results validate the use of *in vitro* approaches for characterizing cell signaling as a preliminary step for further studies *in vivo*.

Our global phosphorylation analysis revealed several regions of interest in the IRS-1 sequence. First, inflammation-mediated hyper-phosphorylation at Ser^{312} has been shown to decrease insulin signaling by interfering with association of the PTB domain (residues 160 – 263) of IRS-1 with the insulin receptor (5,22). Elevated phosphorylation at Ser^{616} and Ser^{636} may interfere with the association of the p85 regulatory subunit of PI 3'-kinase with phospho-YXXM motifs of IRS-1 in this same region (5,15). This may be due to steric factors if the phosphorylated serine residues block access to critical regulatory regions of IRS-1 containing phosphotyrosine residues. Our results indicate that a relatively acute (2 hr.) stimulation with insulin increases phosphorylation at Ser^{312}, Ser^{616}, and Ser^{636}. This could imply that, like Ser^{323}, these sites might not only have negative regulatory roles, but also could play an unknown positive role in the acute, stimulatory phase of insulin action. On the other hand, since chronic high insulin concentrations downregulate IRS-1 protein *in vitro* (23) and induce insulin resistance *in vivo* (33), it is possible that our observations after two hours of insulin infusion reflect the initiation of insulin resistance. Time-course studies will be needed to address these questions.

With respect to phosphorylation of Ser^{616} by insulin, a recent study using immunoblot analysis with a site-specific antibody directed against IRS-1 phosphorylated at Ser^{616} found no effect of insulin on the level of phosphorylation of this site in healthy humans (34). These results contrast with the present mass spectrometry analysis that showed a 2.9 ± 0.8-fold insulin-induced increase in phosphorylation of Ser^{616} (34). This dissimilarity of the results from the different methods was in keeping, however, with our own results for Ser^{312} and $Ser^{636/639}$ in which we showed greater increases in phosphorylation in response to insulin when assessed by mass spectrometry vs. immunoblot analyses. These differences in results from the two methods may result from inherent difficulties in quantification of immunoblots, in particular due to their limited dynamic range.

Phosphorylation at Ser^{1223} interferes with association of the tyrosine phosphatase SHP2 with IRS-1 and enhances insulin signaling by increasing tyrosine phosphorylation of IRS-1 in response to insulin (13). Therefore, insulin-induced phosphorylation at Ser^{1223} could serve as a mechanism to increase insulin action. Increased phosphorylation at Ser^{1101}, in the same general region, also potentially could influence association of SHP2 with IRS-1. One particularly

interesting region of IRS-1 revealed by our analyses (amino acids 328 – 520) contains three phosphorylation sites that are significantly and markedly decreased in response to insulin (Ser^{348}, Thr^{446}, and Thr^{495}). Of note is Thr^{495}, the phosphorylation of which decreases to an almost undetectable level after two hours of physiological hyperinsulinemia. The function of these phosphorylation sites is unknown, but such dramatic changes are unlikely to be without effect.

The potential contribution of insulin-induced downregulation of IRS-1 protein to these results should be considered in light of other reports indicating that chronic insulin exposure can lead to a decrease in IRS-1 protein via phosphorylation, followed by ubiquitination and proteasomal degradation (23). Although the period of exposure to insulin in the present study was more acute than chronic, a modest (30%), albeit not statistically significant, decrease in total IRS-1 protein was observed. Such a small decrease would not substantially affect the estimation of insulin-induced increases or decreases in phosphorylation of particular sites using our MS-based approach. However, it remains possible that large decreases in phosphorylation of certain sites, such as those observed at Ser^{348}, Thr^{446}, and Thr^{495}, could be due to selective degradation of populations of IRS-1 that are phosphorylated at those sites. On extrapolation, this implies that phosphorylation of this region of IRS-1 might target it for ubiquitination and degradation. However, additional experiments are required to elucidate the function of phosphorylation of sites in this region of IRS-1.

Our mass spectrometry-based strategy to quantify site-specific protein phosphorylation presents several advantages over other approaches. First, our method has the ability to detect unknown sites of phosphorylation—such as Thr^{495}. Second, this MS-based technique has the capability of quantifying a large number of phosphorylation sites in IRS-1 from a single biological sample. Third, this approach can be used to study *in vivo* regulation of IRS-1 phosphorylation not only in healthy subjects, but also in populations with specific diseases. For example, it will be important to use this technique to determine whether dysregulation of IRS-1 phosphorylation is involved in insulin resistance. Finally, the method described here not only represents a powerful means to understand the physiological and pathophysiologic relevance of serine and threonine phosphorylation of IRS-1, but it also provides a new tool for quantification of changes in posttranslational modifications of many proteins from small samples of human tissue.

Acknowledgements

The authors thank Ginger Hook for expert nursing assistance and Kenneth Kirschner for outstanding technical assistance. This work was supported by the National Institutes of Health (R01DK047936, R01DK066983) and the American Diabetes Association (Mentor-Based Postdoctoral Fellowship).

References

1. White MF: Insulin signaling in health and disease. *Science* 302:1710-1711, 2003

2. Cusi K, Maezono K, Osman A, Pendergrass M, Patti ME, Pratipanawatr T, DeFronzo RA, Kahn CR, Mandarino LJ: Insulin resistance differentially affects the PI 3-kinase- and MAP kinase-mediated signaling in human muscle. *J Clin Invest* 105:311-320, 2000

3. Krook A, Bjornholm M, Galuska D, Jiang XJ, Fahlman R, Myers MG, Jr., Wallberg-Henriksson H, Zierath JR: Characterization of signal transduction and glucose transport in skeletal muscle from type 2 diabetic patients. *Diabetes* 49:284-292, 2000

4. White MF: IRS proteins and the common path to diabetes. *Am J Physiol Endocrinol Metab* 283:E413-422, 2002

5. Aguirre V, Werner ED, Giraud J, Lee YH, Shoelson SE, White MF: Phosphorylation of Ser307 in insulin receptor substrate-1 blocks interactions with the insulin receptor and inhibits insulin action. *J Biol Chem* 277:1531-1537, 2002

6. Beck A, Moeschel K, Deeg M, Haring HU, Voelter W, Schleicher ED, Lehmann R: Identification of an in vitro insulin receptor substrate-1 phosphorylation site by negative-ion muLC/ES-API-CID-MS hybrid scan technique. *J Am Soc Mass Spectrom* 14:401-405, 2003

7. Gao Z, Hwang D, Bataille F, Lefevre M, York D, Quon MJ, Ye J: Serine phosphorylation of insulin receptor substrate 1 by inhibitor kappa B kinase complex. *J Biol Chem* 277:48115-48121, 2002

8. Greene MW, Garofalo RS: Positive and negative regulatory role of insulin receptor substrate 1 and 2 (IRS-1 and IRS-2) serine/threonine phosphorylation. *Biochemistry* 41:7082-7091, 2002

9. Greene MW, Sakaue H, Wang L, Alessi DR, Roth RA: Modulation of insulin-stimulated degradation of human insulin receptor substrate-1 by Serine 312 phosphorylation. *J Biol Chem* 278:8199-8211, 2003

10. Hartman ME, Villela-Bach M, Chen J, Freund GG: Frap-dependent serine phosphorylation of IRS-1 inhibits IRS-1 tyrosine phosphorylation. *Biochem Biophys Res Commun* 280:776-781, 2001

11. Kim JA, Yeh DC, Ver M, Li Y, Carranza A, Conrads TP, Veenstra TD, Harrington MA, Quon MJ: Phosphorylation of SER 24 in the PH domain of IRS-1 by mPLK/IRAK: Cross-talk between inflammatory signaling and insulin signaling that may contribute to insulin resistance. *J Biol Chem*, 2005

12. Liu YF, Herschkovitz A, Boura-Halfon S, Ronen D, Paz K, Leroith D, Zick Y: Serine phosphorylation proximal to its phosphotyrosine binding domain inhibits insulin receptor substrate 1 function and promotes insulin resistance. *Mol Cell Biol* 24:9668-9681, 2004

13. Luo M, Reyna S, Wang L, Yi Z, Carroll C, Dong LQ, Langlais P, Weintraub ST, Mandarino LJ: Identification of insulin receptor substrate 1 serine/threonine phosphorylation sites using mass spectrometry analysis: regulatory role of serine 1223. *Endocrinology* 146:4410-4416, 2005

14. Moeschel K, Beck A, Weigert C, Lammers R, Kalbacher H, Voelter W, Schleicher ED, Haring HU, Lehmann R: Protein kinase C-zeta-induced phosphorylation of Ser318 in insulin receptor substrate-1 (IRS-1) attenuates the interaction with the insulin receptor and the tyrosine phosphorylation of IRS-1. *J Biol Chem* 279:25157-25163, 2004

15. Mothe I, Van Obberghen E: Phosphorylation of insulin receptor substrate-1 on multiple serine residues, 612, 632, 662, and 731, modulates insulin action. *J Biol Chem* 271:11222-11227, 1996

16. Qiao LY, Zhande R, Jetton TL, Zhou G, Sun XJ: In vivo phosphorylation of insulin receptor substrate 1 at serine 789 by a novel serine kinase in insulin-resistant rodents. *J Biol Chem* 277:26530-26539, 2002

17. Sugita M, Sugita H, Kaneki M: Increased insulin receptor substrate 1 serine phosphorylation and stress-activated protein kinase/c-Jun N-terminal kinase activation associated with vascular insulin resistance in spontaneously hypertensive rats. *Hypertension* 44:484-489, 2004

18. Ueno M, Carvalheira JB, Tambascia RC, Bezerra RM, Amaral ME, Carneiro EM, Folli F, Franchini KG, Saad MJ: Regulation of insulin signalling by hyperinsulinaemia: role of IRS-1/2 serine phosphorylation and the mTOR/p70 S6K pathway. *Diabetologia* 48:506-518, 2005

19. Yi Z, Luo M, Mandarino LJ, Reyna SM, Carroll CA, Weintraub ST: Quantification of phosphorylation of insulin receptor substrate-1 by HPLC-ESI-MS/MS. *J Am Soc Mass Spectrom* 17:562-567, 2006
20. Weigert C, Hennige AM, Brischmann T, Beck A, Moeschel K, Schauble M, Brodbeck K, Haring HU, Schleicher ED, Lehmann R: The phosphorylation of Ser318 of insulin receptor substrate 1 is not per se inhibitory in skeletal muscle cells but is necessary to trigger the attenuation of the insulin-stimulated signal. *J Biol Chem* 280:37393-37399, 2005
21. Yu C, Chen Y, Cline GW, Zhang D, Zong H, Wang Y, Bergeron R, Kim JK, Cushman SW, Cooney GJ, Atcheson B, White MF, Kraegen EW, Shulman GI: Mechanism by which fatty acids inhibit insulin activation of insulin receptor substrate-1 (IRS-1)-associated phosphatidylinositol 3-kinase activity in muscle. *J Biol Chem* 277:50230-50236, 2002
22. Dunaif A: Insulin resistance in women with polycystic ovary syndrome. *Fertil Steril* 86 Suppl 1:S13-14, 2006
23. Pederson TM, Kramer DL, Rondinone CM: Serine/threonine phosphorylation of IRS-1 triggers its degradation: possible regulation by tyrosine phosphorylation. *Diabetes* 50:24-31, 2001
24. DeFronzo RA, Tobin JD, Andres R: Glucose clamp technique: a method for quantifying insulin secretion and resistance. *Am J Physiol* 237:E214-223, 1979
25. Lowry OH, Rosebrough NJ, Farr AL, Randall RJ: Protein measurement with the Folin phenol reagent. *J Biol Chem* 193:265-275, 1951
26. Yi Z, Luo M, Carroll CA, Weintraub ST, Mandarino LJ: Identification of phosphorylation sites in insulin receptor substrate-1 by hypothesis-driven high-performance liquid chromatography-electrospray ionization tandem mass spectrometry. *Anal Chem* 77:5693-5699, 2005
27. Rizza RA, Mandarino LJ, Gerich JE: Dose-response characteristics for effects of insulin on production and utilization of glucose in man. *Am J Physiol* 240:E630-639, 1981
28. Hunter T: Signaling--2000 and beyond. *Cell* 100:113-127, 2000
29. Bouzakri K, Roques M, Gual P, Espinosa S, Guebre-Egziabher F, Riou JP, Laville M, Le Marchand-Brustel Y, Tanti JF, Vidal H: Reduced activation of phosphatidylinositol-3 kinase and increased serine 636 phosphorylation of insulin receptor substrate-1 in primary culture of skeletal muscle cells from patients with type 2 diabetes. *Diabetes* 52:1319-1325, 2003
30. Rui L, Aguirre V, Kim JK, Shulman GI, Lee A, Corbould A, Dunaif A, White MF: Insulin/IGF-1 and TNF-alpha stimulate phosphorylation of IRS-1 at inhibitory Ser307 via distinct pathways. *J Clin Invest* 107:181-189, 2001
31. Greene MW, Morrice N, Garofalo RS, Roth RA: Modulation of human insulin receptor substrate-1 tyrosine phosphorylation by protein kinase Cdelta. *Biochem J* 378:105-116, 2004
32. Paz K, Liu YF, Shorer H, Hemi R, LeRoith D, Quan M, Kanety H, Seger R, Zick Y: Phosphorylation of insulin receptor substrate-1 (IRS-1) by protein kinase B positively regulates IRS-1 function. *J Biol Chem* 274:28816-28822, 1999
33. Iozzo P, Pratipanawatr T, Pijl H, Vogt C, Kumar V, Pipek R, Matsuda M, Mandarino LJ, Cusi KJ, DeFronzo RA: Physiological hyperinsulinemia impairs insulin-stimulated glycogen synthase activity and glycogen synthesis. *Am J Physiol Endocrinol Metab* 280:E712-719, 2001
34. Bouzakri K, Karlsson HK, Vestergaard H, Madsbad S, Christiansen E, Zierath JR: IRS-1 serine phosphorylation and insulin resistance in skeletal muscle from pancreas transplant recipients. *Diabetes* 55:785-791, 2006

Table 1. Subject characteristics.

Gender (F/M)	3/2
Age (yrs.)	27 ± 4
Weight (kg)	70 ± 6
Body Mass Index (kg/m^2)	24 ± 1.4
Fasting Plasma Glucose (mM)	5.0 ± 0.2
Clamp Plasma Glucose (mM)	4.9 ± 0.3
Fasting Plasma Insulin (pmole/l)	84 ± 8
Clamp Plasma Insulin (pmole/l)	506 ± 46
Insulin-Stimulated Glucose Disposal ($mg \cdot kg\ FFM^{-1} \cdot min^{-1}$)	9.0 ± 0.9

Data are given as mean ± SE

.

Table 2. Effect of insulin infusion on phosphorylation of endogenous IRS-1 isolated from muscle biopsies.

Residues	Sequence	Site(s)	Fold Change Due to Insulin
303-325	(R)SRTESITATpSPASM$_{ox}$VGGKPGSFR	Ser^{312}	2.6 ± 0.4*
328-353	(R)ASpSDGEGTM$_{ox}$SRPASVDGSPVSPSTNR	Ser^{330}	1.1 ± 0.2
328-353	(R)ASSDGEGTM$_{ox}$SRPASVDGSPVpSPSTNR	Ser^{348}	0.4 ± 0.1*
444-457	(R)SVpTPDSLGHTPPAR	Thr^{446}	0.2 ± 0.1*
494-520	(R)CpTPGTGLGTSPALAGDEAASAADLDNR	Thr^{495}	0.1 ± 0.1*
573-580	(R)HpSAFVPTR	Ser^{574}	1.1 ± 0.1
596-626	(R)GGHHRPDSSTLHTDDGYM$_{ox}$PM$_{ox}$pSPGVAPVPSGR	Ser^{616}	2.9 ± 0.8*
627-638	(R)KGpSGDYM$_{ox}$PM$_{ox}$SPK	Ser^{629}	1.2 ± 0.1
627-638	(R)KGSGDYM$_{ox}$PM$_{ox}$pSPK	Ser^{636}	2.1 ± 0.3*
892-922	(PK)pSPGEYVNIEFGSDQSGYLSGPVAFHSSPSVR	Ser^{892}	1.6 ± 0.1*
999-1016	(R)QSYVDTpSPAAPVSYADM$_{ox}$R	Ser^{1005}	0.3 ± 0.2*
1075-1081	(R)VNLpSPNR	Ser^{1078}	1.1 ± 0.1
1098-1112	(R)RHpSSETFSSTPSATR	Ser^{1100}	0.8 ± 0.2
1099-1112	(R)HSpSETFSSTPSATR	Ser^{1101}	1.3 ± 0.1*
1221-1236	(R)RSpSEDLSAYASISFQK	Ser^{1223}	1.3 ± 0.1*
Singly-phosphorylated peptides not separated by HPLC			
303-325	(R)SRTEpSITATSPASM$_{ox}$VGGKPGpSFR	Ser^{307}	**
303-325	(R)SRTESITATSPASM$_{ox}$VGGKPGpSFR	Ser^{323}	**
525-538	(R)THpSAGTSPTITHQK	Ser^{527}	**
525-538	(R)THSAGTpSPTITHQK	Ser^{531}	**
1141-1161	(R)HpSSASFENVWLRPGELGGAPK	Ser^{1142}	**
1141-1161	(R)HSpSASFENVWLRPGELGGAPK	Ser^{1143}	**
1141-1161	(R)HSSApSFENVWLRPGELGGAPK	Ser^{1145}	**

Data are shown as fold change compared to basal (before insulin infusion values—see text for calculations) and are presented as mean ± SEM of four independent experiments. Each experiment represents the average of two replicates from the same muscle homogenate. *, $P < 0.05$ by paired t-test (basal vs. insulin, comparing normalized ion intensities); pS, phosphoserine; pT, phosphothreonine; M_{ox}, oxidized methionine. ******Monophosphorylated peptides were not sufficiently separated by HPLC to permit individual quantification (see text). Evidence for the existence of modification at each site was obtained by tandem mass spectrometry.

Figure Legends

Figure 1. Representative coverage map of peptides detected in tryptic digests of human muscle IRS-1 using HPLC-nanospray-LTQ-FT/ICR analysis. Detected peptides are shown in red, phosphorylation sites are shown in green. Underlined sequences are known SH2 recognition motifs (YXXM/L/I).

Figure 2. Reconstructed ion current chromatograms corresponding to three phosphopeptides detected in tryptic digests of IRS-1 isolated from human muscle biopsies of a representative healthy control subject taken one hour before (Basal) and at the end of two hours of insulin infusion (Insulin) during a euglycemic, hyperinsulinemic clamp. Upper panel, GGHHRPDSSTLHTDDGYM$_{ox}$PM$_{ox}$pSPGVAPVPSGR [*m/z* 1109.82 (3+); IRS-1$^{596-626}$; the abundance of this phosphopeptide increased after 2-hr insulin infusion compared to basal; mean fold-change ± SEM of four independent experiments, 2.9 ± 0.8 ($P < 0.05$)]; middle panel, VNLpSPNR [*m/z* 440.21 (2+); IRS-1$^{1075-1081}$; no change after 2-hr insulin infusion]; lower panel, ASSDGEGTM$_{ox}$SRPASVDGSPVpSPSTNR [*m/z* 882.38 (3+); IRS-1$^{328-353}$; the abundance of this phosphopeptide decreased after 2-hr insulin infusion; mean fold-change ± SEM of four independent experiments, 0.4 ± 0.1 ($P < 0.05$)].

Figure 3. Identification of sites of phosphorylation in an hIRS-1 peptide that was detected in two distinct mono-phosphorylated forms in tryptic digests of IRS-1 isolated from a human muscle biopsy. A, Reconstructed ion current chromatogram for *m/z* 705.3 illustrating chromatographic separation of IRS-1$^{627-638}$ KGSGDYM$_{ox}$PM$_{ox}$pSPK (pSer^{636}) and KGpSGDYMoxPMoxSPK (pSer^{629}). B, tandem mass spectrum of pSer^{636} peptide; C, tandem mass spectrum of pSer^{629} peptide; *, loss of H_3PO_4 (98 u) from the indicated fragment; §, loss of $SOCH_4$ (64 u); M_{ox}, oxidized methionine. Ion annotations shown in italics indicate fragments that contain phosphate. In panel B, the presence of y-series ions containing phosphate starting with y_4 support phosphorylation of Ser^{636}. The shift of b_5 from *m/z* 445.2 in panel B to *m/z* 525.1 in panel C, corresponding phospho-containing b_7 and b_9 ions and the absence of modification for y-series ions until y_{10} indicate phosphorylation at Ser^{629}.

Figure 4. Relative changes in phosphorylation of specific sites in IRS-1 produced by insulin during a euglycemic, hyperinsulinemic clamp. Insulin-stimulated changes relative to basal values are expressed as the base-2 log of the change, so a 100% increase corresponds to a value of 1.0 and a 50% decrease is -1.0; for sites where there was no change in relative phosphorylation, the value is zero. The amino acid residue number for each site of phosphorylation is given on the x-axis, and the positions of the pleckstrin homology (PH) and phosphotyrosine binding (PTB) domains are shown in gray. The insulin receptor, PI 3'-kinase, and SHP2 are shown contiguous to their binding regions.

Figure 5. Immunoprecipitation and immunoblot analysis of homogenates of biopsies of *vastus lateralis* muscle taken one hour before (Lane 1) and at the end of two hours of insulin infusion (Lane 2) during a euglycemic, hyperinsulinemic clamp in a representative healthy control subject. Muscle homogenates (1 mg protein for anti-pSer$^{636/639}$, anti-pSer^{312} and anti-phosphotyrosine; 0.3 mg for total IRS-1 protein) were immunoprecipitated using anti-IRS-1 antibody as described in the text. Immunoprecipitated proteins were resolved on SDS-polyacrylamide gels and the proteins were transferred electrophoretically to nitrocellulose

membranes. The membranes were exposed to anti-phosphotyrosine (top panel), anti-IRS-1 $pSer^{636/639}$ (second panel), anti-IRS-1 $pSer^{312}$ (third panel), or anti-IRS-1 protein (lower panel) antibodies and visualized by chemiluminescence.

Online Appendix 1 (A-R). Tandem mass spectra of phosphopeptides detected in tryptic digests of IRS-1 isolated from biopsies of human *vastus lateralis* muscle; *, loss of H_3PO_4 (98 u) from the indicated fragment; §, loss of $SOCH_4$ (64 u); $^{\Delta}$, loss of H_2O (18 u); M_{ox}, oxidized methionine. All sites were verified manually by comparison with fragmentation patterns generated *in silico*.

Online Appendix 2. Reconstructed ion chromatograms corresponding to the six representative IRS-1 peptides that were reproducibly detected in tryptic digests of IRS-1 isolated from human muscle biopsies. The traces shown here are from biopsies of a representative healthy control subject taken one hour before (Basal) and at the end of two hours of insulin infusion (Insulin) during a euglycemic, hyperinsulinemic clamp; r.t., retention time; r.r.t, relative retention time compared to Ang II. There was no significant change of total IRS-1 abundance after the 2-hr insulin infusion compared to basal.

Online Appendix 3. Reconstructed ion chromatograms illustrating chromatographic separation of mono-phosphorylated $IRS\text{-}1^{328\text{-}353}$ peptide analogs. A, *m/z* 882.4; B, fragmentation of *m/z* 882.4 to *m/z* 937.5, a unique ion in the tandem mass spectrum of $IRS\text{-}1^{328\text{-}353}$ phosphorylated at Ser^{348}; B, fragmentation of *m/z* 882.4 to *m/z* 1010.3, a unique ion in the tandem mass spectrum of $IRS\text{-}1^{328\text{-}353}$ phosphorylated at Ser^{330}. Tandem mass spectra of $IRS\text{-}1^{328\text{-}353}$ phosphorylated at Ser^{330} and Ser^{348} are shown in Online Appendix 1C and 1D, respectively.

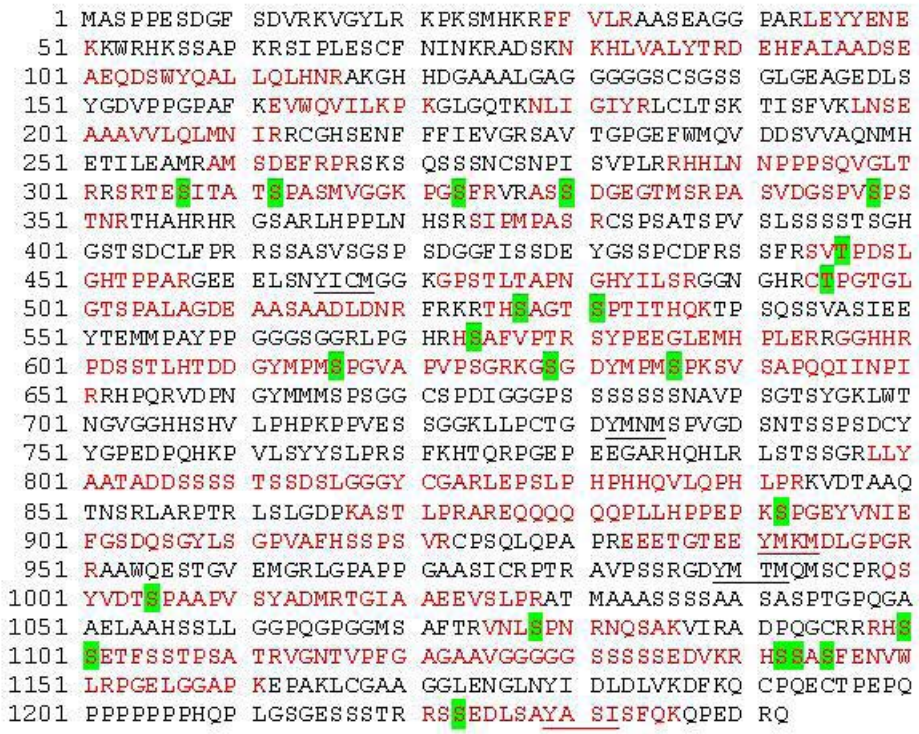
1 MASPPESDGF SDVRKVGYLR KPKSMHKRFF VLRAASEAGG PARLEYYENE
51 KKWRHKSSAP KRSIPLESCF NINKRADSKN KHLVALYTRD EHFAIAADSE
101 AEQDSWYQAL LQLHNRAKGH HDGAAALGAG GGGGSCSGSS GLGEAGEDLS
151 YGDVPPGPAF KEVWQVILKP KGLGQTKNLI GIYRLCLTSK TISFVKLNSE
201 AAAVVLQLMN IRRCGHSENF FFIEVGRSAV TGPGEFWMQV DDSVVAQNMH
251 ETILEAMRAM SDEFRPRSKS QSSSNCSNPI SVPLRRHHLN NPPPSQVGLT
301 RRSRTESITA TSPASMVGGK PGSFRVRASS DGEGTMSRPA SVDGSPVSPS
351 TNRTHAHRHR GSARLHPPLN HSRSIPMPAS RCSPSATSPV SLSSSSTSGH
401 GSTSDCLFPR RSSASVSGSP SDGGFISSDE YGSSPCDFRS SFRSVTPDSL
451 GHTPPARGEE ELSNYICMGG KGPSTLTAPN GHYILSRGGN GHRCTPGTGL
501 GTSPALAGDE AASAADLDNR FRKRTHSAGT SPTITHQKTP SQSSVASIEE
551 YTEMMPAYPP GGGSGGRLPG HRHSAFVPTR SYPEEGLEMH PLERRGGHHR
601 PDSSTLHTDD GYMPMSPGVA PVPSGRKGSG DYMPMSPKSV SAPQQIINPI
651 RRHPQRVDPN GYMMMSPSGG CSPDIGGGPS SSSSSSNAVP SGTSYGKLWT
701 NGVGGHHSHV LPHPKPPVES SGGKLLPCTG DYMNMSPVGD SNTSSPSDCY
751 YGPEDPQHKP VLSYYSLPRS FKHTQRPGEP EEGARHQHLR LSTSSGRLLY
801 AATADDSSSS TSSDSLGGGY CGARLEPSLP HPHHQVLQPH LPRKVDTAAQ
851 TNSRLARPTR LSLGDPKAST LPRAREQQQQ QQPLLHPPEP KSPGEYVNIE
901 FGSDQSGYLS GPVAFHSSPS VRCPSQLQPA PREEETGTEE YMKMDLGPGR
951 RAAWQESTGV EMGRLGPAPP GAASICRPTR AVPSSRGDYM TMQMSCPRQS
1001 YVDTSPAAPV SYADMRTGIA AEEVSLPRAT MAAASSSSAA SASPTGPQGA
1051 AELAAHSSLL GGPQGPGGMS AFTRVNLSPN RNQSAKVIRA DPQGCRRRHS
1101 SETFSSTPSA TRVGNTVPFG AGAAVGGGGG SSSSSEDVKR HSSASFENVW
1151 LRPGELGGAP KEPAKLCGAA GGLENGLNYI DLDLVKDFKQ CPQECTPEPQ
1201 PPPPPPPHQP LGSGESSSTR RSSEDLSAYA SISFQKQPED RQ

Figure 1

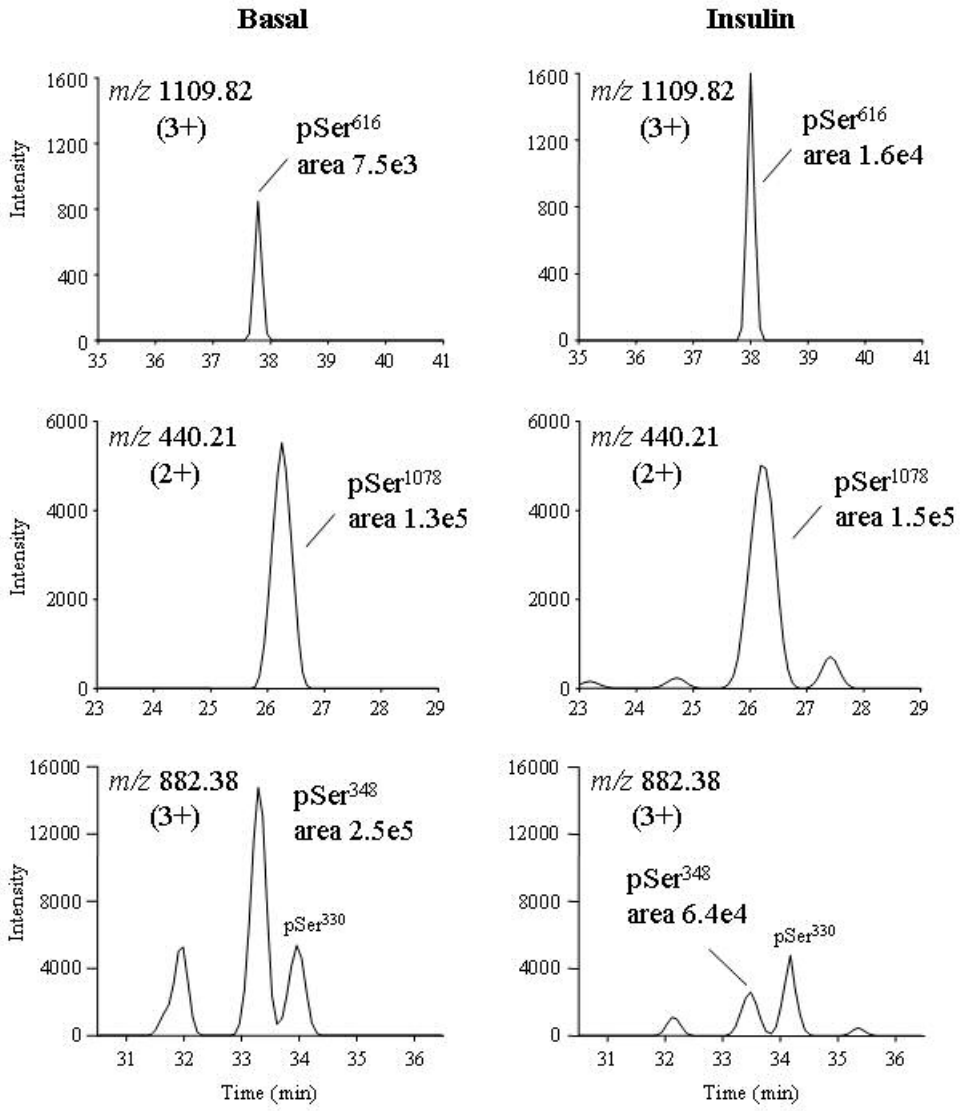
Basal
Insulin
m/z 1109.82
(3+)
pSer616
area 7.5e3
m/z 1109.82
(3+)
pSer616
area 1.6e4
m/z 440.21
(2+)
pSer1078
area 1.3e5
m/z 440.21
(2+)
pSer1078
area 1.5e5
m/z 882.38
(3+)
pSer348
area 2.5e5
pSer330
m/z 882.38
(3+)
pSer348
area 6.4e4
pSer330
Intensity
Time (min)

Figure 2

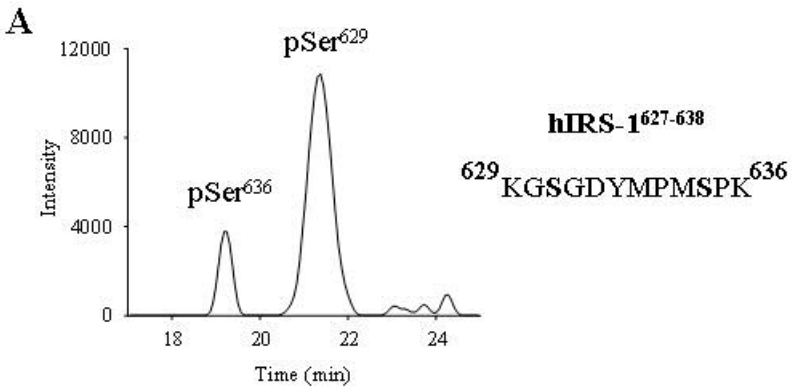
A
12000
8000
4000
0
Intensity
pSer629
pSer636
18
20
22
24
Time (min)
hIRS-1627-638
629KGSGDYMPMSPK636

Figure 3

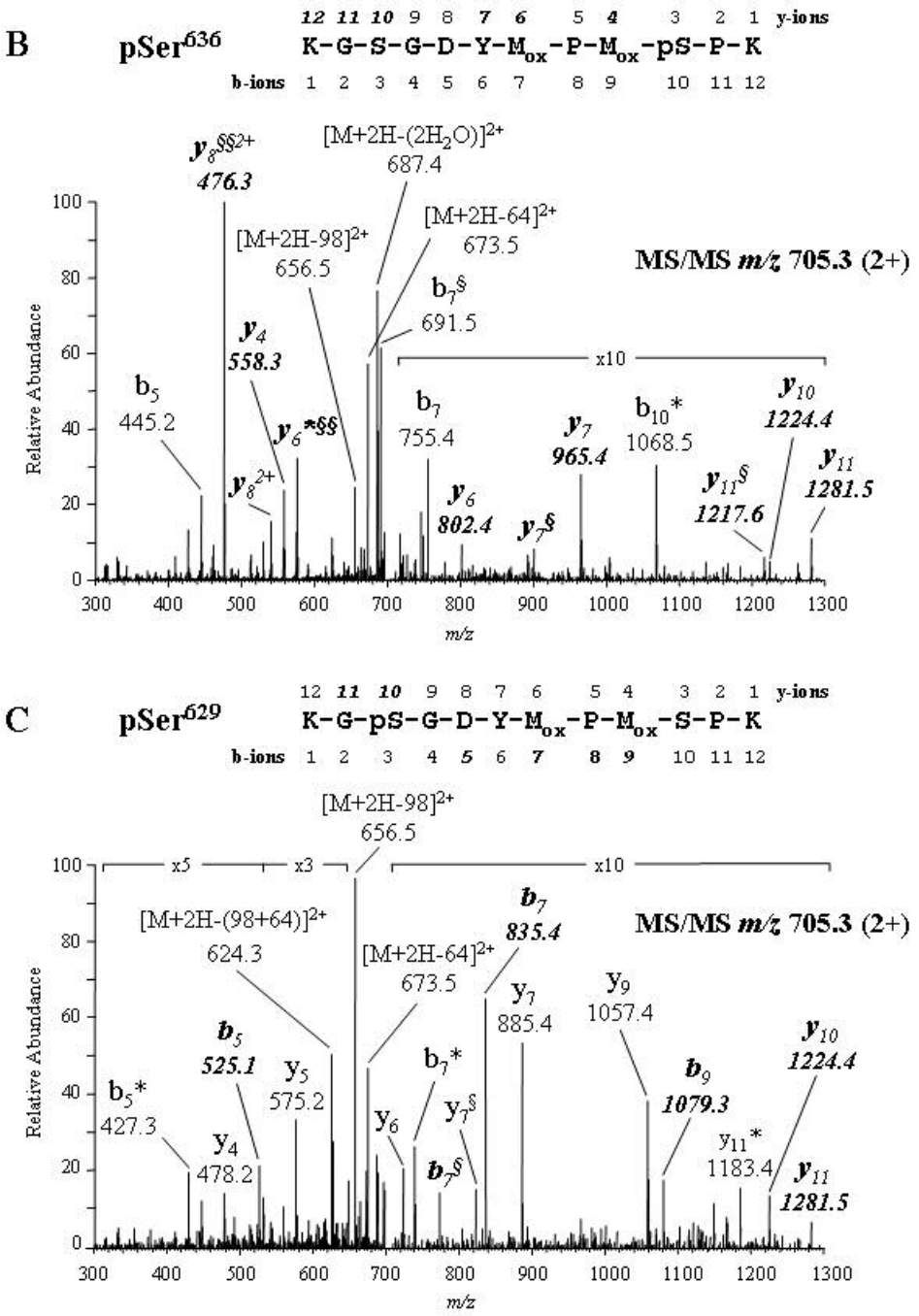
B
pSer636
12 11 10 9 8 7 6 5 4 3 2 1 y-ions
K-G-S-G-D-Y-Mox-P-Mox-pS-P-K
b-ions 1 2 3 4 5 6 7 8 9 10 11 12
MS/MS m/z 705.3 (2+)
Relative Abundance
m/z
C
pSer629
12 11 10 9 8 7 6 5 4 3 2 1 y-ions
K-G-pS-G-D-Y-Mox-P-Mox-S-P-K
b-ions 1 2 3 4 5 6 7 8 9 10 11 12
MS/MS m/z 705.3 (2+)
Relative Abundance
m/z

Figure 3

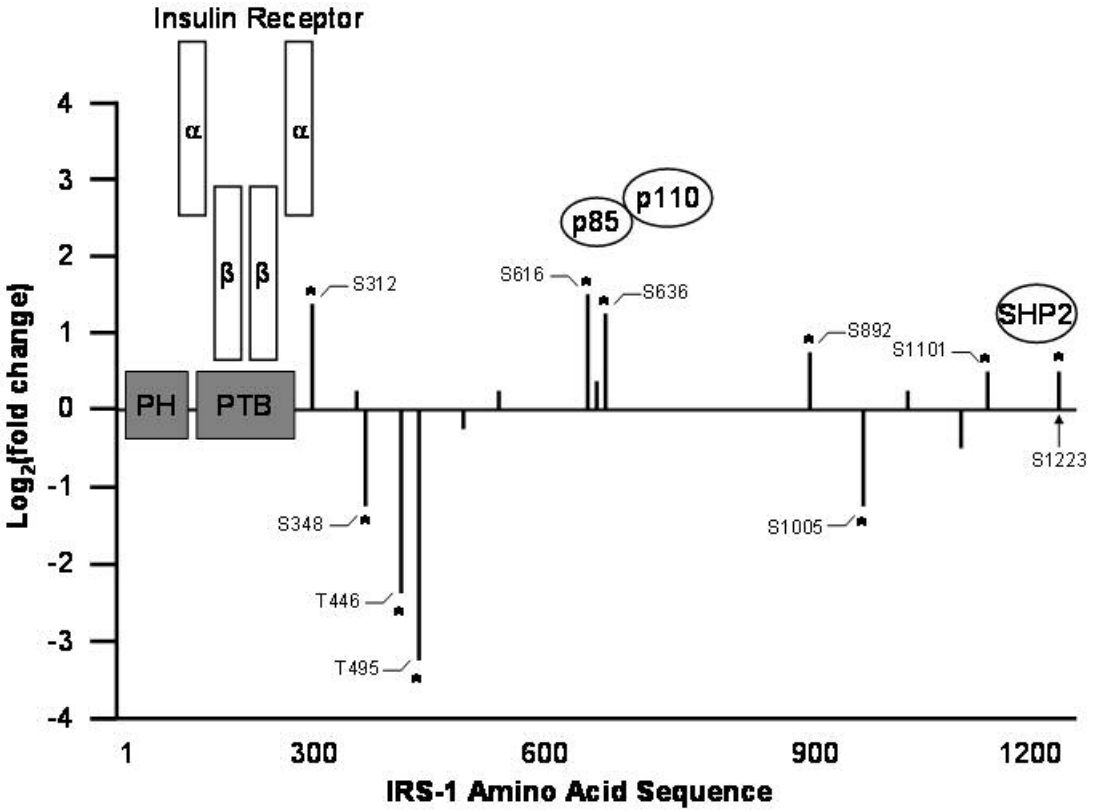
Insulin Receptor
α
α
β
β
p85
p110
SHP2
PH
PTB
S312
S348
T446
T495
S616
S636
S892
S1005
S1101
S1223
Log2(fold change)
4
3
2
1
0
-1
-2
-3
-4
1
300
600
900
1200
IRS-1 Amino Acid Sequence

Figure 4

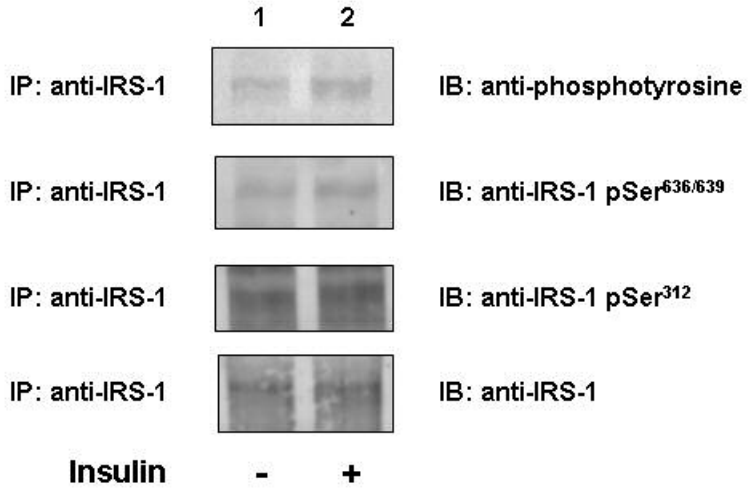
1
2
IP: anti-IRS-1
IB: anti-phosphotyrosine
IP: anti-IRS-1
IB: anti-IRS-1 pSer636/639
IP: anti-IRS-1
IB: anti-IRS-1 pSer312
IP: anti-IRS-1
IB: anti-IRS-1
Insulin
-
+

Figure 5